A&A 475, 677–684 (2007)
DOI: 10.1051/0004-6361:20077429

Astronomy & Astrophysics

X-ray emission from A-type stars⋆

C. Schröder and J. H. M. M. Schmitt

Hamburger Sternwarte, Universität Hamburg, Gojenbergsweg 112, 21029 Hamburg, Germany
e-mail: cschroeder@hs.uni-hamburg.de

Received 7 March 2007 / Accepted 10 September 2007

ABSTRACT

Being fully radiative, stars of spectral type A are not expected to harbor magnetic dynamos and hence such stars are not expected to produce X-ray emission. Indeed, while the X-ray detection rate of such stars in X-ray surveys is low, it is not zero and some of the brighter A-type stars have been detected on different occasions and with different instruments. To study systematically the puzzle of the X-ray emitting A-type stars, we carried out an X-ray study of all A-type stars listed in the Bright Star Catalogue using the ROSAT public data archive. We found a total of 312 bright A-type stars positionally associated with ROSAT X-ray sources; we analyzed the X-ray light curves as well as searched for evidence of RV variations to identify possible late-type companions producing the X-ray emission. In this paper we present a list of X-ray active A-type stars, including the collected data about multiplicity, X-ray luminosity and spectral peculiarities.

Key words. X-rays: stars – stars: activity – stars: coronae – stars: general

1. Introduction

Many if not all late-type, main-sequence stars are surrounded by X-ray emitting coronae. Extensive ROSAT surveys (Schmitt & Liefke 2004) show that the X-ray detection rates among the brighter late-type stars with spectral type F and later are approaching 100%; the same holds for early-type stars surveyed by Berghöfer et al. (1996, 1997), although the X-ray production mechanisms in the early-type stars is thought to be fundamentally different from that in late-type stars. The X-ray production mechanism for the late-type stars is believed to be similar to that of the Sun, and indeed, the dramatic increase in X-ray detection rates for stars thought to possess surface convection zones lends support to the idea that the stellar magnetism, which is ultimately held responsible for the observed activity phenomena, is generated in the turbulent outer layers of late-type stars. Early-type stars on the other hand produce strong radiatively driven winds, and instabilities in these winds are thought to be ultimately responsible for the ubiquitous X-ray emission observed from these stars. A general paucity of X-ray emission among (late-type) B- and especially A-type stars has been noticed ever since the days of the *Einstein Observatory* (Schmitt et al. 1985). Since A-type stars have neither convection zones nor do they have – at least – strong winds, none of the X-ray production mechanisms operating in early- or late-type stars ought to be operating and therefore A-type stars are "expected" to be intrinsically X-ray dark.

This expectation of intrinsic X-ray darkness/weakness is borne out by the available X-ray data on nearby A-type stars. The nearest A-type stars are Sirius and Vega, but the signals seen in the ROSAT X-ray detectors (especially the ROSAT-HRI) are in all likelihood produced by UV-radiation rather than genuine X-ray radiation (Zombeck et al. 1997; Berghöfer et al. 1999). A further, and more severe problem for the interpretation of X-ray data from A-type stars is binarity. Because of the ubiquity of X-ray emission among late-type stars, all A-type stars with a late-type companion should be X-ray sources, which are simply attributable to the presence of late-type companions. Since such optically, possibly quite faint, companions are easy to hide in the vicinity of an optically bright A-type star, the X-ray emission from even presumably single A-type stars could in fact attributed to previously unknown late-type companions. Because of the rather short main sequence life times of A-type stars late-type companions of such stars are still considered young, hence most of the "hidden" late-type companions are expected to be X-ray bright and active sources.

One of the unique attributions of the observed X-ray emission in a stellar system is quite difficult; it requires X-ray data with sufficient angular resolution, which would actually still be insufficient to rule out close companions. Stelzer et al. (2006) used Chandra imaging observations to spatially resolve a sample of main sequence B-type stars with recently discovered companions at arcsecond separation. They found that all spatially resolved companions are X-ray emitters, but – somewhat surprisingly – seven out of eleven B-type stars were also found to be X-ray sources. Obviously this result still does not rule out additional close companions of the B stars in the system, but would imply a rather large binary frequency of intermediate-mass stars and a high number of systems with more than two components.

Another technique is observing systems with a special viewing geometry such as an eclipsing binary. Schmitt & Kürster (1993) and Schmitt (1998) studied the (totally) eclipsing binary α CrB, consisting of an A0V primary and a G2V secondary. At secondary optical minimum with the optically bright A-type star in front of the optically fainter G-type star a total X-ray eclipse was observed, thus demonstrating, first, that the A-type primary is indeed X-ray dark "as expected", and second, that the size of the X-ray corona around the secondary is at least smaller than the size of the primary.

In a few other cases, the correct attribution of observed X-ray emission from A-type stars can be made using the spectral

⋆ Tables 2 et 3 are only available in electronic form at http://www.aanda.org

information contained in the X-ray data. In the prototypical case β Crt (Fleming et al. 1991) the soft PSPC spectrum suggested the presence of an X-ray emitting white dwarf, which was subsequently confirmed (Barstow et al. 1994; Vennes et al. 1998). Thus β Crt is very similar to the binary system Sirius AB with its prototypical white dwarf; if this system was ten times further away from the Sun, it would still be quite X-ray bright, but the B component would be almost impossible to detect at least at optical wavelengths.

Obviously the set of – for whatever reasons – X-ray bright A-type stars is a bewildering zoo of quite different beasts. The purpose of this paper is to provide a definitive summary of the ROSAT observations of bright A-type stars. If the puzzle of X-ray emitting A-type stars is ever to be solved, a well defined sample of the brightest of such objects is required. The X-ray emitting A-type stars were detected and identified and an extensive literature search was carried out to single out those objects whose X-ray emission cannot be explained by emission from late-type companions, at least with the currently available information on these objects.

2. Observations and data analysis

2.1. Data basis

The ROSAT Observatory was operated between 1990–1998. Between July 1990 and January 1991 it carried out its ROSAT All-Sky Survey (RASS) with the ROSAT Position Sensitive Proportional Counter (PSPC). Afterwards pointed observations of individual objects were carried out within the framework of the ROSAT guest investigator program both with the PSPC and a High (angular) Resolution Imager (HRI). These detectors had fields of view of about 7000 arcmin^2 for the PSPC and 1000 arcmin^2 for the HRI, so that many X-ray sources were picked up serendipitously in the field of view of many observations, whose original scientific goal was actually quite different.

2.1.1. X-ray data

The results of both the RASS observations and the ROSAT pointed observations are available in the ROSAT results archive in the form of source lists. Four of the five catalogs were used for the present study, i.e., the ROSAT Bright Source and Faint Source Catalog, the Second ROSAT Source Catalog of Pointed Observations with the PSPC and the First ROSAT Source Catalog of Pointed Observations with the HRI. These catalogs as well as detailed information on the detection and screening procedures applied in the construction of the catalogs are available via www from the ROSAT Home Page at Max-Planck-Institut für extraterrestrische Physik (`http://wave.xray.mpe.mpg.de/rosat/catalogue`) or its mirror sites. Altogether, these catalogs contain 372 896 entries. From the data provided by these catalogs we extracted position and count rates of those sources, which can be positionally associated with bright A-type stars. For those sources observed with the PSPC with the RASS, we used the X-ray luminosities derived by Hünsch et al. (1998).

2.1.2. Optical data

As our source of optical data we used the 5th version of the Bright Star Catalog (BSC) by Hoffleit & Jaschek (1991), which contains 9110 objects of magnitude 6.5 or brighter. For the parallax values we used the data given in the Hipparcos database. Out of those 9110 objects, 1966 stars are listed as A-type stars in the BSC. The BSC thus constitutes a very large and complete database of bright A-type stars with a lot of auxiliary information about its entries. For information concerning possible hidden late-type companions of the A-type stars we used the SIMBAD database extensively.

2.1.3. Catalogs

The catalogs in Tables 2 and 3 present the main result of our efforts; in Table 2 we provide optical and X-ray data of 84 detected "bona fide" single A-type stars as contained in the BSC. Table 3 shows the same data for 228 X-ray associated A-type stars that are members of known binary or multiple systems or show signs of hidden companions. The columns of the table contain the following information:

Col. 1: HR number, taken from the BSC;
Col. 2: binary flag; S means single star, B visual or eclipsing binary, SB spectroscopic binary, PB potential binary;
Col. 3: rotational velocity in km s^{-1};
Col. 4: separation for visual binary systems;
Col. 5: difference in the magnitude between the A star and its closest companion;
Col. 6: MK spectral types of the components;
Col. 7: distance of the star as given by Hipparcos parallaxes;
Col. 8: catalog flag indicating in which observation mode the star has been observed; r means ROSAT all-sky survey, p PSPC pointing and h HRI pointing;
Col. 9: mean count rate of the associated X-ray source; first choice were PSPC pointing source data, second HRI and third survey observation data;
Col. 10: error of the count rate; errors with a value of 0.0 mark sources with flags in the ROSAT catalogs that indicate a suspect source or false detection in the field;
Col. 11: X-ray luminosity derived from the distance as given in Col. 7 and the count rates as given in Col. 9. The values are given in units of 10^{27} erg/s.

2.2. Data analysis

2.2.1. Correlation of the catalogs

For the correlation between the X-ray and the optical source lists we combined the ROSAT Faint Source Catalog and the ROSAT Bright Source Catalog to the RASS catalog. The resulting three X-ray catalogs and the Bright Star Catalog were searched for positional coincidences. As a matching criterion we used 90 arcsec for survey data, 36 arcsec for pointing data with the PSPC and 18 arcsec for HRI data. The differently chosen positional acceptance thresholds reflect the fact that the intrinsic positional accuracy of survey data, and the PSPC and HRI pointing data increases in that order. In Fig. 1 we plot histograms showing the number of sources obtained by our positional correlation analysis as a function of angular distance. The concentration of the sources towards the target positions, i.e., the 1966 A-type stars in the BSC catalog, is obvious. As shown in Fig. 1 the matching criteria approximately mark the distances at which the probability of obtaining a spurious X-ray source becomes greater than the chance to obtain a correct identification. Therefore the chosen values for the acceptance thresholds do not introduce significant errors into our list of seemingly X-ray active A-type stars.

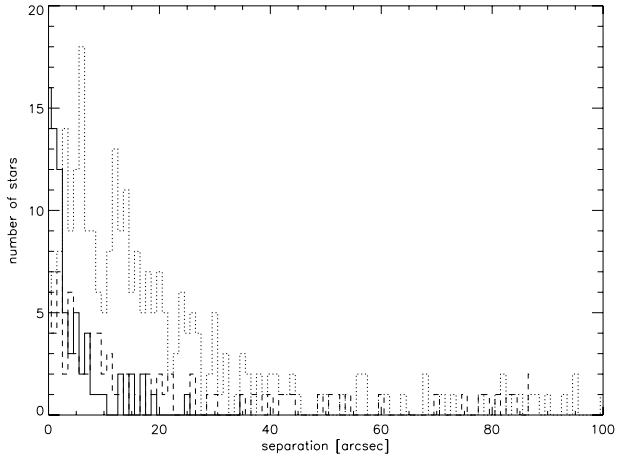

Fig. 1. Number of A-type stars at a given separation between the optical position of the star and the position of the associated X-ray source. The dotted line shows the data for the BSC-RASS correlation, the dashed line represents the BSC-PSPC data and the solid line those from the BSC-HRI correlation.

2.2.2. Search for late-type companions

The most common explanation for seemingly X-ray active A-type stars is to assume that the X-ray emission does not originate from the A-type star itself but rather from a low mass (binary) companion. To check this hypothesis we searched for signatures of hidden companions in four ways. First, we examined possible variations in the radial velocity and proper motion of the A-type star given in the SIMBAD database and accordant papers. Second, we checked the ROSAT X-ray light curves for flare-like variations which might be an indicator of the presence of a late-type companion. Third, for those stars observed in more than one observation mode we performed a comparison of the count rates in the different observations to check for long time scale variability. Different count rates at the two different observation times are an indicator for a variable source and therefore hint at the presence of a hidden companion. Admittedly, the significance of this indicator is small, since the possible mechanisms for the X-ray emission from A-type star are somewhat speculative. Finally, another, albeit only weak, indicator is the rotational velocity of the A-type star itself. Given enough time to synchronize their orbits, the members of a binary system would rotate slowly and a high rotational velocity might therefore indicate a single star or a young binary system. The results of these tests are included in our list of seemingly X-ray active A-type stars. Stars without any available information on binarity and no signatures of hidden companions we consider as bona fide single stars.

3. Results

On basis of the correlation of the Bright Star Catalogue and the three ROSAT catalogs we can associate 312 of the 1966 A-type stars with one or more X-ray sources. In total, 272 of these sources are listed as RASS detected X-ray sources, 63 sources are listed in the PSPC pointing catalog and 69 have been observed at the highest possible angular resolution with the ROSAT HRI. The total number of these sources is larger than 312 because some stars have been detected in more than one mode/instrument.

Table 1. Statistics of spectral peculiar A-stars.

	Total	X-ray detected	Known binaries	Binaries among X-ray detections
A-type stars	1966	312 (16%)	733 (37%)	194 (62%)
Am	212	41 (19%)	89 (42%)	34 (83%)
Ap	133	18 (14%)	51 (38%)	8 (44%)
A giants	474	62 (13%)	179 (38%)	35 (56%)

3.1. Spurious identifications

We stress that all our X-ray source identifications are obtained solely on the basis of positional coincidence. Despite of this we expect the number of spurious identifications to be very small. Calculating the number of identifications obtained by distributing approximately 120 000 RASS sources over 1966 positions (i.e., the number of A-type stars contained in the BSC) with a detected cell radius of 90 arcsec results in 11 spurious identifications or 4% of the total number of RASS detections of A-type stars. The actual distribution of position offsets is much narrower (cf., Fig. 1). To be specific, only 4 out of our 272 survey detections have position offsets of more than 50 arcsec, and only 11 X-ray detections are off by more than 30 arcsec from the optical positions of the A-type star. We thus conclude that the fraction of incorrectly identified X-ray emitters in our sample is at the one to two percent level and that the overwhelming majority of our sources are correctly identified with an optically bright A-type star.

3.2. Detection statistics

Next we divide the 1966 A-type stars as listed in the BSC into four subgroups according to their spectral features: Am, Ap, giant and main sequence stars. To check whether the X-ray activity of A-type stars depends on this grouping we determined the fraction of X-ray active stars in all of the different subgroups. In Table 1 we list the total number of A-type stars, the number of seemingly X-ray active stars, the number of known binary or multiple systems and the binary frequency among the X-ray active stars.

Given the count statistics there are obviously no significant differences in the fraction of X-ray active stars between the different subgroups. However, the X-ray detection rates among the known binaries are larger than the binary fraction in the corresponding subsamples. We interpret this strong increase of the binary frequency in the X-ray active subsamples as an indicator for a larger number of binary systems. These systems, which can be optically separated in quite a number of cases, cannot be separated in the ROSAT X-ray data and therefore cause possibly false correlations between the A-type star and the X-ray source (i.e. the companion). Clearly, the number of known binaries among all A-type stars has to be considered a lower limit. While the sample of seemingly X-ray active stars was intensively searched for signatures of binarity, the remaining 1654 A-type stars, which have not been detected in X-rays, have been classified only according to the multiplicity information given in the BSC.

3.3. Detection rate vs. spectral type

In Fig. 2 we plot the detection rate of A-type stars vs. spectral type. As is obvious from Fig. 2, the mean percentage of X-ray

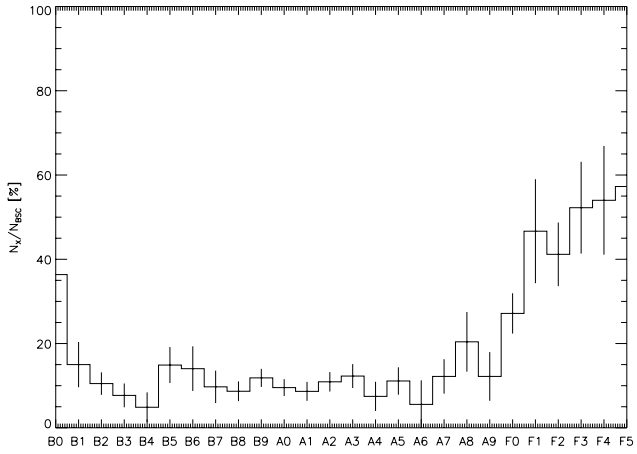

Fig. 2. Percentage of X-ray active stars N_x from the total number of stars N_{BSC} of a given spectral type. Note the strong increase in the X-ray detection rates for stars in the range A9–F3.

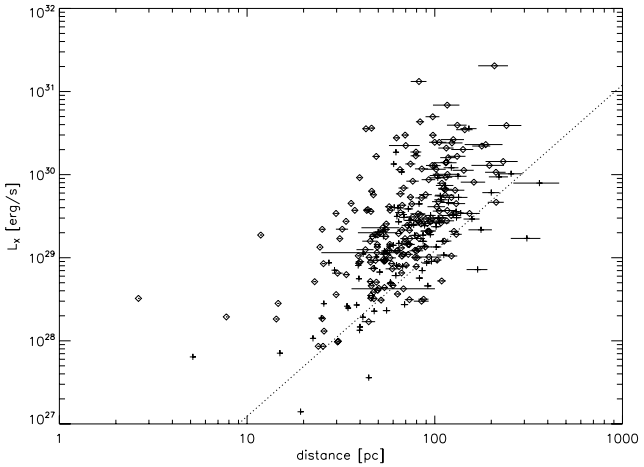

Fig. 3. L_x vs. distance for the 312 A-type stars associated with a ROSAT X-ray source. The crosses indicate single stars, and the diamonds known or possible multiple systems. The dotted line represents the typical detection limit for the RASS observations, i.e., $f_X \approx 10^{-13}$ erg cm^{-2} s^{-1}.

active stars among the stars with spectral type A0 to A9 is 10% to 15%. This is consistent with the X-ray activity frequency in the above mentioned special subgroups in Table 1. The onset of convection and hence the presumed onset of an $\alpha\Omega$ − dynamo at spectral type A9–F3 and the radiation driven winds at early B-type stars are clearly visible. The fact that less than 60% of the F5 stars are X-ray active in our data we attribute to the flux limit of the X-ray data; if instead, one considers a volume-limited sample of F-type stars (Schmitt & Liefke 2004), one finds a detection rate of essentially 100%.

3.4. X-ray luminosity

Figure 3 shows the X-ray luminosity of the ROSAT sources associated with the 312 X-ray detected A-type stars as a function of stellar distance; the parallaxes for the stars have been taken from the Hipparcos catalog (ESA 1997). The two objects with the faintest X-ray sources are the AV5 star β Pictoris (HD 39060) and the AV7 star δ Doradus (HD 39014). In the case of β Pictoris the recorded ROSAT HRI signal is completely consistent with being due to UV contamination (Hempel et al. 2005), in the case of δ Doradus this is extremely likely. Berghöfer et al. (1999) derived a relation between the U, B and V magnitudes and the HRI count rates. The predicted count rate for δ Doradus of 0.24 cts/ks corresponds to the observed HRI count rate of 0.63 cts/ks within the errors. The dotted line represents the typical detection limit for the RASS observations, i.e., $f_X \approx 10^{-13}$ erg cm^{-2} s^{-1}. Sources with a lower L_X have been observed with the PSPC or HRI via pointing mode, resulting in deeper observations with lower detection limits. Figure 3 suggests the single and double stars from our X-ray detected sample do not possess significantly different X-ray luminosities as a function of distance.

The distribution functions of the X-ray luminosities of single and binary stars are shown in Fig. 4. Carrying out a formal test with a one-sided Kolmogorov-Smirnov test allows us to reject the null hypothesis that in both classes the X-ray originate from the same population, with a significance of 95%, according to a maximum difference of 0.158 between the two distributions. Additional bootstrap tests with two artificial samples of randomly chosen X-ray detected stars and the same size as the original samples do not support this high level of significance. Out of 10 000 runs 2127 show distributions in which the maximum difference between the distributions is larger than the measured value of 0.158, hence the bootstrap test suggests only an 80% confidence for the rejection of the hypothesis that the two samples originate from the same population. We note that the offset in the cumulative distribution function might be a result of a observational bias. The problem is that binary systems with an A-type star and a low mass companion are harder to resolve than systems with a higher mass companion and therefore more likely to be misidentified as a single star. For solar-like companions this would create a "single star" sample with lower X-ray luminosity, since L_X scales with L_{bol}. This effect might be negated by the fact that for M-type stars, especially young ones which are to be expected in binary systems with A-type stars, the difference in X-ray luminosity vanishes (Stauffer et al. 1994; Stern et al. 1995; Randich et al. 1996).

3.5. Completeness

Since the absolute magnitudes of our sample stars vary quite a lot, our sample is definitely not volume-limited. Considering a distance limit of 50 parsecs our sample is definitely complete in the sense that all A-type stars up to that distance are sample members. Furthermore, since from the typical RASS flux limit we can compute the RASS upper X-ray luminosity limit of $ul = 2.4 \times 10^{25} \times d_{pc}2$ erg/s, which translates into an X-ray luminosity of $L_X = 6 \times 10^{28}$ erg/s, and thus the X-ray luminosity distribution faction above that limit is unaffected by any non-detections. In the 50 pc volume there are 220 cataloged A-type stars, out of which 82 (or 37%) are associated with an X-ray source; in other words, the observed detection rate in a volume-limited sample of A-type stars significantly exceeds 15%. The upper limits to the X-ray luminosity of most of the 138 non-detections are in the range $\approx 10^{28}$ erg/s for the RASS data; a few nearby A-type stars with upper limits from dedicated pointings (Schmitt 1997; Pease et al. 2006) have upper limits considerably below this value; these stars include α Lyr (A0V), β Leo (A3V) and α PsA (A3V). Out of these 82 X-ray detcted stars, 60 objects (or 73% of the X-ray detected stars) are known or supposed to have one or more companions, while 22 stars (or 27%) of the X-ray detected stars are "bona fide" single stars. The cumulative

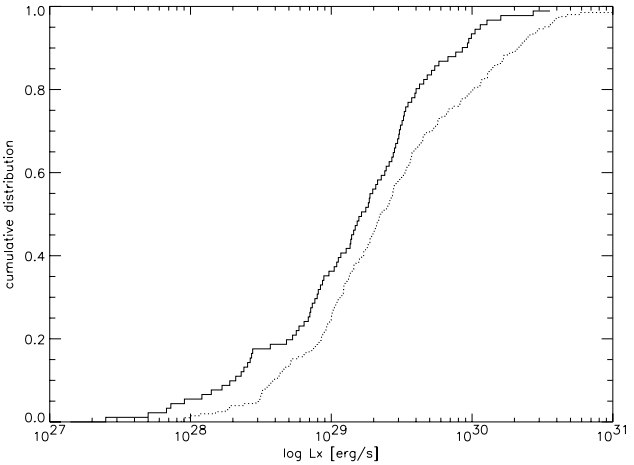

Fig. 4. Cumulative distribution function of the X-ray luminosity for the single star sample (solid line) and binary star sample (dotted line). The null hypothesis that both samples originate from the same distribution can be rejected with a significance of 95%.

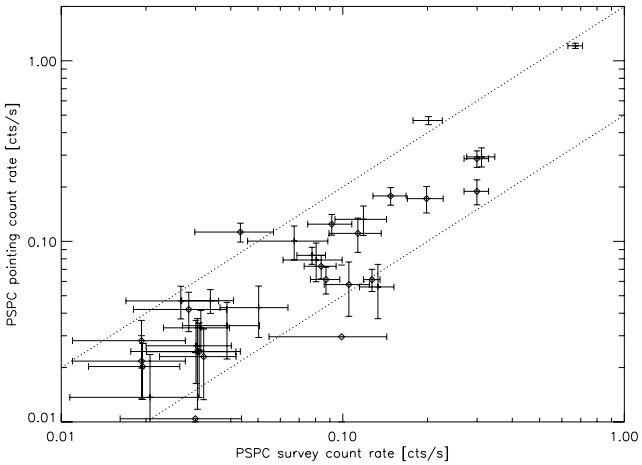

Fig. 5. Comparison of X-ray count rates for 35 stars detected both in the all-sky survey and the PSPC pointing program. The two dotted lines indicate a factor 2 variation from unity. Single and double stars are represented by crosses and diamonds respectively. Stars with large deviations from the regression line are identified.

distribution functions of the 22 single stars and 60 known binary stars shows a comparable offset as the samples presented in Sect. 3.5, they do of course, suffer from the same possible bias(es). Thus we conclude that a volume-limited sample yields similar properties for X-ray detected A-type stars, except that the true detection rate maybe quite a bit higher.

3.6. Variability between survey and pointing data

For some of our sample stars multiple X-ray detections are available from RASS data, the ROSAT PSPC pointing or HRI pointing program. The time span between survey and pointed observations with the PSPC is typically of the order of 1–2 years with larger time spans between the survey and the pointed observations carried out with the HRI instrument.

In Fig. 5 we plot the PSPC count rate observed during the all-sky survey vs. the PSPC count rate observed during the pointing program in a double-logarithmic representation for those of our sample stars detected in both observing modes. The two dotted lines indicate a factor of two deviation above and below unity. As Fig. 5 shows, all count rates lie within this area according to their error bars. Variations by a factor of 4 are not uncommon for active late-type stars and would therefore support the late-type companion hypothesis, as does the fact that there is no significant difference in the variability of single and binary stars.

The variability between the count rates obtained during the PSPC pointed observations and the HRI pointed observations is shown in Fig. 6. Again, the dotted lines mark a factor of two deviation above and below "unity"; "unity" in this case accounts for the fact that the ROSAT-HRI instrument is less sensitive than the ROSAT-PSPC leading to an HRI count rate typically a quarter of the PSPC count rate. Only HR 5999 shows a variation in count rate differing by a factor of 12; however, we suspect that the X-ray emission originates from the possible T Tauri star Rossiter 3930, which is separated to HR 5999 by 1.3″ (Zinnecker & Preibisch 1994; Stecklum et al. 1995), also, HR 5999 lies in a crowded field not resolved in the survey data.

Figure 7 shows the third possible combination of the three catalog data sets, the comparison of the count rates obtained during the PSPC survey program and the HRI pointing program. As in Fig. 6, the dotted line indicates "unity" which takes into account the lower sensitivity of the ROSAT-HRI instrument. Five stars show apparent count rate variations. HR 1189 is a binary system with a separation of 8″, containing an A1V and a late B-type star. Due to the fact that the survey observation has an exposure time of only 70 s, it is most likely that the variation originates from the uncertainty in the count rate of the RASS source. HR 2890 (Castor B) is a spectroscopic binary with spectral types of A5Vm and early M (Gudel & Schmitt 1996). Closeby, with a separation of 3.9″, lies the spectroscopic binary system Castor A, which is composed of an A1V and a late K-star. Due to the configuration of these two binary systems the X-ray emission and its variability can be clearly associated with the late-type companions of the A-type stars (Güdel et al. 2001). HR 3524 (RS Cha) is an eclipsing binary consisting of two A8V stars (Andersen 1975). In contrast to earlier publications, Mamajek et al. (2000) derived ages of 5.0×106 and 4.3×106 yr for the two components and suggest that this system, because of the fact that the X-ray emission of RS Cha shows flare-like variations, is actually a triple system with an undetected T Tauri star. According to the Washington Visual Double Star Catalog, HR 8662 is a visual binary with a separation of 10.5″ and additionally the A component is a spectroscopic binary. Corbally (1994) specifies the spectral type of the B component as G9V, thus giving a likely explanation for the count rate variations, keeping in mind the resolving power during the survey observations.

3.7. Individual objects of pointed HRI observations

In the following we present some ROSAT HRI observations of X-ray detected A-type stars for which PSPC and high resolution ROSAT HRI observations are available. Additionally, detailed information about these stars has been published in different papers and might give hints about the absence or presence of undetected late-type companions.

All of the HRI observations presented here show very small deviations between the optical position of the A-type star and the position of the associated X-ray source. The values range from less than 1″ to 5″ which is less than the spatial resolution of the HRI. All of the discussed stars are single stars or binary systems with a separation which is large enough to be resolved by the

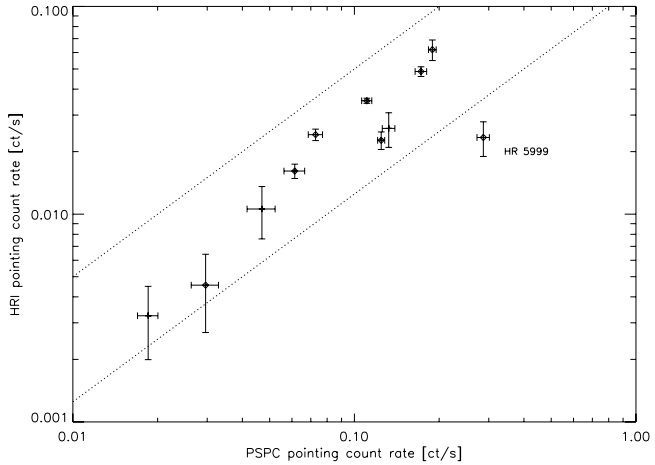

Fig. 6. Comparison of X-ray count rates for 14 stars detected both in the PSPC pointing program and the HRI pointing program. The two dotted lines indicate a factor 2 variation from unity. Single and double stars are represented by crosses and diamonds respectively. Stars with large deviations from the regression line are identified.

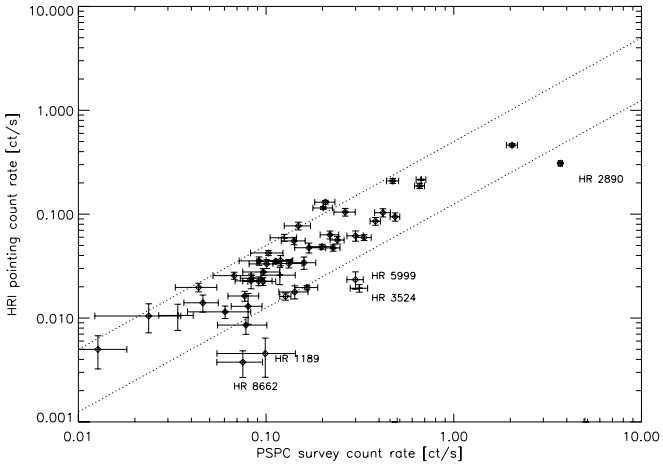

Fig. 7. Comparison of X-ray count rates for 55 stars detected both in the PSPC survey program and the HRI pointing program. The two dotted lines indicate a factor 2 variation from unity. Single and double stars are represented by crosses and diamonds respectively. Stars with large deviations from the regression line are identified.

HRI. Objects with associated X-ray source near the edge of the detector, and therefore less accurate positions, are also excluded.

3.7.1. HR 191

This system is a visual binary with a separation of 19.8″, according to the Washington Visual Double Star Catalog, with spectral types of A0IV and K2-5V. Two HRI observations of HR 191 have been carried out, one in 1991 with an exposure time of 2.1 ks and a second in 1995 with 5.3 ks. Both observations show a weak X-ray source near the position of HR 191. While the K-star could not be detected in the first observation in 1991, a weak source is found at the position of the K-star in 1995, possibly due to a flare. The positional deviations of the X-ray sources with respect to their optical counterparts are less than one arcsecond for both stars. Unfortunately, the count rate of the A-star associated source is too low and the exposure time is too short for a significant statistical test for variability, which would be an indicator for the presence of a hidden late-type companion. The X-ray luminosity of 1.7×10^{29} erg/s is in the range that can be explained by an active late-type companion and indeed, Gerbaldi et al. (1999) mention this star as a possible astrometric binary.

3.7.2. HR 433

As for the previous system, HR 433 is a binary system composed of an A0V and an early K-star. The separation is 22″ and the deviation of the position of the X-ray source from the A-type star is about 5″. Only one source was found in the X-ray observations with an exposure time of 4.8 ks. While an X-ray luminosity of 1.1×10^{29} erg/s is clearly consistent with an active late-type star, the statistical variability tests show no significant signature of variability, which would have indicated such a hidden active late-type star. The values for the radial velocity vary from −7 to 12 km s^{-1}, and this might be a hint for a yet undetected companion.

3.7.3. HR 778

The Hipparcos Catalog lists this A6V star as a potential astrometric binary with a short period, but no other publication gives any information about a possible companion. The only X-ray source in the HRI image is separated from the optical position of the A-type by less than one arcsecond. During the observations, which took place in July 1997 (5.4 ks) and December 1997 and January 1998 (27.6 ks combined) the L_X of 1.7×10^{28} erg/s led to count rates which were too low for statistical tests of variability. The two measurements of the radial velocity give consistent values of 3 km s^{-1}.

3.7.4. HR 789

HR 789 is again a visual binary system consisting of A2V primary accompanied by an early M dwarf with a separation of 24″. The ROSAT HRI image with an exposure time of 1.5 ks, presented in Fig. 8., clearly shows two X-ray sources at the optical positions of the stars, with the brighter X-ray source being associated with the position of the A-type star. While the Kolmogorov test showed no clear signs of variability, an additional χ^2 test gives a probability of less than 5% that this source is constant. The L_x of 9.2×10^{29} erg/s is consistent with an active late-type star. The rotational velocity of 190 km s^{-1} contradicts a synchronously rotating companion, but Buscombe & Morris (1961) found variations in the radial velocity leading to the possibility of a non-synchronously rotating companion.

3.7.5. HR 2174

This A3V star is a member of a triple system with its closest companion at a distance of 29.2″. Only one source was found near the optical position of the A-type star. During the two HRI observations in March 1995 (1.8 ks) and March 1996 (3.8 ks) this X-ray source has a deviation of one and two arcseconds to the optical position of HR 2174 and is therefore associated with the A-type star. As in the two cases mentioned above, the count rates are too low and the exposure times are too short to allow any significant statements about the variability of the X-ray

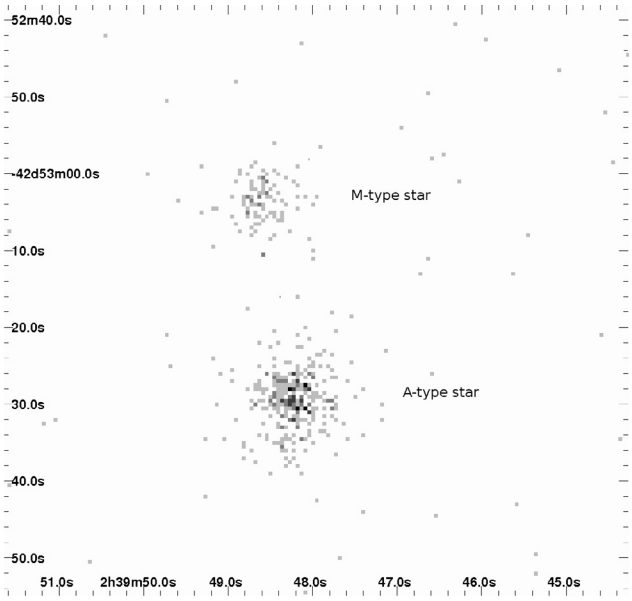

Fig. 8. ROSAT-HRI image of HR 789. The separation between the brighter X-ray source and the optical position of the A-type star is about an arcsecond.

source. With 2.3×10^{30} erg/s the X-ray luminosity is at the upper limit for late-type stars. The fast rotational and constant radial velocity are indicators against an undetected companion.

3.7.6. HR 3321

This star is an A5III-IV star with no known companion. The HRI observations took place during April 1998 and show one X-ray source, separated by 3″ from the optical position of HR 3321. The combined exposure time of the three observation blocks is 6.4 ks. The statistical test shows a significant variability during one of these observations. Additionally, the value of the rotational velocity is 11 km s^{-1} and therefore too low to be an indicator against a late-type companion. The radial velocity is constant at a value of 27.3 km s^{-1}.

3.7.7. HR 6681

This A0V star is a member of a triple system with a separation of 20.8″ from its closest companion, most likely an early G-type star. In the ROSAT HRI observations with an exposure time of 2.9 ks carried out in September 1994, two X-ray sources with a separation of 16″ are visible and the position of the brighter X-ray source agrees with the optical position of the A-type star to better than 3″. The statistical test showed no significant signs for or against variability and measurements of the radial velocity have not been carried out so far.

3.7.8. HR 8463

HR 8463 is an A5V star and a member of a quadruple system with a separation of 23.2″ from its nearest companion. Two X-ray sources are detected in the vicinity of the A-type star and the weaker source has a deviation of less than an arcsecond to the optical position of the A-type star. The observation is divided in four parts with a total exposure time of 6.4 ks; in three of them statistical tests do not show any signs of variability and in the forth one the tests do not give a significant result. With a distance of 55 pc and a count rate of 0.021 ± 0.002 cts/s the L_X amounts to 1.8×10^{29} erg/s. The varying values for the radial velocity of −2 to −16.2 km s^{-1} might be an indicator for a companion.

3.8. Further comments on HRI observations

From the six known and optically separated binary systems two companions have not been found in the observations, even though the separation of the stars is large enough to be resolved by the HRI. The reason for this is most likely the fact that at a distance of 67 pc in the case of HR 433 and 186 pc for HR 2174 late-type stars are hardly detectable, even in a very active state.

HR 2015 is a single star separated from a X-ray source by less than 3″. This source is listed in the HRI catalog but could not be found by our source-detection routines. We therefore flagged HR 2015 as an uncertain candidate and excluded it from the previous discussion.

4. Summary and conclusion

The correlation of the Bright Star Catalogue with the ROSAT X-ray catalogs results in a list of 312 bright A-type stars which can be positionally associated with an X-ray source. The overall ROSAT detection rate of bright A-type stars lies between 10–15% in the spectral range A0–A9, with a steep increase in detection rates among F-type stars. Those 312 A-type stars whose associated X-ray sources are listed in the ROSAT all-sky survey or the pointed observations catalog have been further investigated for signatures of the presence of late-type companions.

As a result of the evaluation of the distribution of seemingly X-ray active stars in the different spectral subgroups it is obvious that there is neither a connection between the spectral type and the frequency of X-ray active stars nor an indication for a connection between spectral peculiarities and X-ray activity. On closer inspection, this is no real surprise. Due to the fact that a significant portion of the observed X-ray emission comes, without much doubt, from late-type companions and these companions are distributed equally on the different spectral classes, a concentration of X-ray activity on a few spectral classes would indeed be astonishing. Otherwise an increased X-ray frequency in a group of spectral peculiar stars would have given a hint about a possible mechanism for X-ray production, such as in the magnetically-confined wind shock model proposed by Babel & Montmerle (1997). Actually none of these subgroups showed an significant increase in the X-ray detection frequency.

The examination of the count rates showed that most of the sources lack sufficient signal to obtain unambiguous results in a variability analysis. The reason for this is the fact that most of the available HRI observations are short snapshots of up to 5 ksec to check if the target is X-ray active at all. Of the presented individual candidates, only the lightcurves of HR 789 and HR 3321 showed significant signs of variability while the lightcurve of HR 8463 was constant in three of four observation periods. We mention in passing that even clear signs of variability do not rule out the possibility that the X-ray source is the A star itself. Due to the absence of a conclusive theory for an X-ray producing mechanism at A-type stars, it is hard to predict if the A stars are variable X-ray sources or not.

For many of the X-ray detected A-type stars, information on binarity exists in partly ambiguous and partly unambiguous forms. A total of 84 of the detected X-ray stars are, however, either bona fide single stars (meaning that no information on binarity and no indications of hidden companions are available),

or resolved multiple stars, implying that at least a third system component must exist, if the X-ray emission is not attributed to the A-type star. These 84 bona fide single stars are therefore particularly well suited candidates for follow-up observations, for example, for high resolution X-ray and IR observations to separate the suggested companion from the A-type star or radial velocity monitoring to search for companions. The list presented here may serve as a starting point for such a project.

References

Andersen, J. 1975, A&A, 44, 445
Babel, J., & Montmerle, T. 1997, A&A, 323, 121
Barstow, M. A., Holberg, J. B., Fleming, T. A., et al. 1994, MNRAS, 270, 499
Berghöfer, T. W., Schmitt, J. H. M. M., & Cassinelli, J. P. 1996, A&AS, 118, 481
Berghöfer, T. W., Schmitt, J. H. M. M., Danner, R., & Cassinelli, J. P. 1997, A&A, 322, 167
Berghöfer, T. W., Schmitt, J. H. M. M., & Hünsch, M. 1999, A&A, 342, L17
Buscombe, W., & Morris, P. M. 1961, MNRAS, 123, 233
Corbally, C. J. 1994, VizieR Online Data Catalog, 3117, 0
ESA 1997, VizieR Online Data Catalog, 1239, 0
Fleming, T. A., Schmitt, J. H. M. M., Barstow, M. A., & Mittaz, J. P. D. 1991, A&A, 246, L47
Gerbaldi, M., Faraggiana, R., Burnage, R., et al. 1999, A&AS, 137, 273
Gudel, M., & Schmitt, J. B. M. M. 1996, in Radio Emission from the Stars and the Sun, ed. A. R. Taylor, & J. M. Paredes, ASP Conf. Ser., 93, 315
Güdel, M., Audard, M., Magee, H., et al. 2001, A&A, 365, L344
Hamaguchi, K., Yamauchi, S., & Koyama, K. 2005, ApJ, 618, 360
Hempel, M., Robrade, J., Ness, J.-U., & Schmitt, J. H. M. M. 2005, A&A, 440, 727
Hoffleit, D., & Jaschek, C. 1991, The Bright star catalogue (New Haven, Conn.: Yale University Observatory), 5th rev. Ed., ed. D. Hoffleit, & C. Jaschek,
Mamajek, E. E., Lawson, W. A., & Feigelson, E. D. 2000, ApJ, 544, 356
Pease, D. O., Drake, J. J., & Kashyap, V. L. 2006, ApJ, 636, 426
Randich, S., Schmitt, J. H. M. M., Prosser, C. F., & Stauffer, J. R. 1996, A&A, 305, 785
Schmitt, J. H. M. M. 1997, A&A, 318, 215
Schmitt, J. H. M. M. 1998, A&A, 333, 199
Schmitt, J. H. M. M., & Kürster, M. 1993, Science, 262, 215
Schmitt, J. H. M. M., & Liefke, C. 2004, A&A, 417, 651
Schmitt, J. H. M. M., Golub, L., Harnden, Jr., F. R., et al. 1985, ApJ, 290, 307
Simon, T., Drake, S. A., & Kim, P. D. 1995, PASP, 107, 1034
Stauffer, J. R., Caillault, J.-P., Gagne, M., Prosser, C. F., & Hartmann, L. W. 1994, ApJS, 91, 625
Stecklum, B., Eckart, A., Henning, T., & Loewe, M. 1995, A&A, 296, 463
Stelzer, B., Huélamo, N., Micela, G., & Hubrig, S. 2006, A&A, 452, 1001
Stern, R. A., Schmitt, J. H. M. M., & Kahabka, P. T. 1995, ApJ, 448, 683
Vennes, S., Christian, D. J., & Thorstensen, J. R. 1998, ApJ, 502, 763
Zinnecker, H., & Preibisch, T. 1994, A&A, 292, 152
Zombeck, M. V., Barbera, M., Collura, A., & Murray, S. S. 1997, ApJ, 487, L69

Online Material

Table 2. List of X-ray associated "bona fide" single or resolved multiple A-type stars.

HR	Binary	$v \sin(i)$	Sep.	δ Mag	Components	Distance	Catalog			CR	±CR	L_{x27}
191	B		20	7	A0IV+K2-5V	74	R		H	0.01147	0.00158	270
378	S	100–112			A3V	67	R			0.01713	0.00787	78.3
398	S				A0Vnn	158	R			0.01228	0.00537	292.1
433	B		22	5	A0V+K0V	68	R		H	0.00856	0.00159	353.3
710	B	23–31	12	3.5	A6Vsp+G5-8V	66	R		H	0.03550	0.00327	422.6
778	PB				A6V	44		P	H	0.01851	0.00154	21
789	B		24	10	A2V+M2-5V	40	R		H	0.2090	0.01200	924
817	S				A1V	107	R			0.04391	0.01295	554.6
943	S	80–90			A5V	58	R			0.04234	0.01681	137.9
1014	S	79			A3V	58		P		0.02082	0.00226	50.2
1039	S	65			A0Vs	104	R			0.03048	0.01085	299.9
1196	S	35–44			A5m	60	R			0.04111	0.01120	141.0
1314	S	230–249			A2Vn	108	R			0.03234	0.00957	498.5
1700	S				A1V	130	R			0.01966	0.00737	358.0
1706	B		12.6/14.6	6/3	A9IV+K2+F+WD	82	R		H	5.051	0.1068	13211.6
1732	S	40–49			A0pSi	137		P		0.02576	0.00168	343.7
1940	S	14-15			A8Vs	41	R			0.01679	0.00761	19.2
2174	B		29.2/..	1.2/3.2	A3V+A0	187	R		H	0.02279	0.00366	3351
2180	S	225–264			A0Vn	78	R			0.02316	0.00804	185.8
2209	S	220–238			A0Vn	54	R			0.04748	0.01412	120.4
2265	S	249			A2-3V	62	R			0.5004	0.02675	1858.1
2350	S				A5V	69		P		0.00796	0.00059	27.3
2351	S	35–44			A9IV	61	R	P		0.05592	0.0	402.3
2658	S				A0V	125	R			0.02326	0.00855	329.1
2683	S				A0pSi	87	R			0.02306	0.00863	186.7
2709	S	62			A0III	255	R			0.02186	0.00799	1023.4
2720	S				A8V	48	R			0.05062	0.01390	74.6
2776	S	83–94			A7s	34	R			0.03516	0.01172	24.8
2869	S	214			A1IV	106	R			0.02414	0.01043	267.7
3131	S	177–245			A1V	73	R			0.03230	0.01504	280.6
3321	S	11–13			A5III-IV	53	R		H	0.02777	0.00213	223.7
3401	S	230–254			A2Vn	110	R			0.01488	0.00712	156.7
3649	S	21–29			A9IVDel Del	51	R			0.03393	0.01188	67.2
3761	S	249			A3Vn	68	R			0.05223	0.01440	331.3
4263	S				A0pSiCr	152	R			0.1431	0.02499	3577.0
4502	S	0–19			A0V	64	R			0.09110	0.02831	270.8
4554	S	163–178			A0VSB	26	R	P		0.04295	0.00349	28.0
4680	S	135–180			A9.5III	55		P		0.01051	0.00094	23.1
4886	S	215–233			A7V	112		P		0.01200	0.0	107.6
4889	S				A7III	48	R	P		0.01368	0.0	22.7
4893	B		22		A1IIIshe.+HR4892	93	R		H	0.00499	0.00176	101.9
4971	S				A9III-IV	62	R			0.02244	0.00843	61
5040	S	18–26			A2m	64	R			0.1240	0.02372	398.1
5062	S	210–248			A5V	25	R	P		0.04679	0.0	18.8
5069	S				Ap SrEuCr	88	R			0.03570	0.01525	137.2
5107	S	178–222			A3V	22	R			0.02536	0.01250	10.7
5216	S	70–81			A3V	83	R			0.07485	0.01343	444.9
5343	S	96			A8III	49		P		0.00597	0.00092	10.3
5357	S	230			A2Vn	68	R			0.05173	0.01835	305.7
5406	S	90–102			A2IV	72	R			0.07643	0.02048	387.0
5468	S	85–96			A1V	60	R			0.3418	0.03006	1341.9
5491	S				Am	64	R			0.04996	0.01835	148.7
5511	S	265–334			A0V	39	R			0.04499	0.01307	55.9
5729	S				A2V	67	R			0.2684	0.03963	1077.2
5759	S	55–65			A3m	92	R			0.00757	0.00353	45.8
5845	S	68–78			A2m	53	R	P		0.1003	0.00477	181.0
5870	S	120–133			A3V	77	R			0.03756	0.01185	247.8
6081	S				A4II/III	361		P		0.00849	0.00187	790.8
6153	S				A7pSrEuCr	54		P		0.05472	0.00462	113.4
6332	S	21–29			A3IV	90	R			0.00731	0.00380	86.4
6386	S	15–23			A0V	114	R			0.03536	0.01261	740.6
6537	S				A0V	118	R			0.04082	0.0189	461.9
6539	S				A0V	104	R	P		0.07882	0.0	915.0
6681	B		20.8/33.7	2.2/6.5	A0V+G0-2V	76	R		H	0.01784	0.00258	950.9
6782	B		14.2		A3V	51	R		H	0.4866	0.0	81
7012	S				A5IV-V	29	R			0.09705	0.03182	70.8
7018	S	30			A0V	131	R			0.01584	0.00307	303.6
7085	S	90–102			A1V	176		P		0.00967	0.00291	216.6
7250	S	35–44			A4III	102	R			0.01807	0.00725	134.8
7312	S	55–64			A9V	27	R			0.1271	0.00981	86.9
7384	S	170–186			A0V	123	R			0.07768	0.01714	1210.4
7416	S				A0p(CrEuSr)	134	R			0.03580	0.01333	532.1
7423	S	165–180			A3V	95	R			0.01309	0.00464	189.8
7498	S				A4III	42	R			0.08967	0.03027	111
7634	S	175			A4Vn	86	R			0.01048	0.00380	70.1
7702	S	190–207			A3V	200	R			0.01118	0.00461	607.6
7730	S		337		A5IIIn	220	R			0.02710	0.00671	939.9
7734	S	220–238			A0V	310		P		0.00248	0.00068	170.7
7826	S				A3V	83	R			0.02057	0.00765	56.9
8463	B		23.2/	5/	A5V	55	R		H	0.02248	0.00192	219.6
8578	S	45–81			A2m	63	R			0.02248	0.00584	81.1
8675	S				A3V	40		P		0.01243	0.00206	13.4
9060	S				A1IV	63	R			0.07669	0.01949	314.3

Table 2. continued.

HR	binary	$v \sin(i)$	sep.	δ mag	Components	Distance	Catalog	CR	±CR	L_{x27}
9062	S	187–191			A1V	49	R	0.05986	0.01889	102.2

Table 3. List of X-ray associated A-type stars in binary or multiple systems or with hints of hidden companions.

HR	Binary	$v \sin(i)$	Sep.	δ Mag	Components	Distance	Catalog			CR	±CR	L_{x27}
104	SB				A3m+F0V	81	R			0.03230	0.01111	281.7
127	B			1.2	A2V+F0-1V	53		P		0.02874	0.0	229.5
196	B		2	10	A2Vs+M2-5V	108	R			0.02738	0.00988	303.1
273	SB				A+A	115	R			0.03753	0.01084	1404.7
325	S	70–100			A3III	72	R			0.03847	0.01332	147.2
328	PB	135–149			A3V	49	R			0.06896	0.01929	143.9
361	B		20/1	1/6	A7IV+F0-1+	45	R			0.09316	0.01655	158.2
428	S	75–86			A2Vs	87	R			0.02676	0.00829	157.4
499	B		1+13	1.4+0.3	A3V+F0-5	79	R			0.2440	0.03439	1685.7
526	B		2	0.6	A3V+A2-5V+.	102	R			0.03084	0.01243	275.9
575	SB			2.1	A3IV+?	36	R		H	0.08562	0.00733	451.1
579	B		5	3	A5III+ F	111	R			0.01921	0.00677	684.1
707	SB		0.5/1.9		A5pSr	43	R		H	0.04733	0.00328	372.1
803	B		3+50	4+5.5	A3V+G5-8V	108	R			0.02129	0.00961	262.5
804	B		2.7	3.8	A3V+G5-8V	25	R			0.3764	0.04390	219.9
815	B				A3V+K0IV	63	R	P	H	1.211	0.02160	2771.5
820	B		1.5+30	2+7	A9V+G2-5V	47	R			0.03485	0.00914	74.2
853	B		<1	3.8	A0V+G5V	100	R			0.1296	0.01978	1283.4
884	PB				A2.5V	145	R		H	0.05928	0.00468	3472
971	S	15–23			A1Vs	133	R			0.03695	0.01026	954.9
976	SB		30.8	5.7	A1m	67	R			0.05050	0.01219	215.8
1019	B		4.4	3.8	A0V	162	R			0.02790	0.00945	811.7
1042	PB	136			A1IV	100	R			0.1748	0.03913	2452.1
1189	B		7	0.6	A1V+G2-5V	49	R	P	H	0.02961	0.00328	134.7
1211	SB		7/165	1.4/7	A2V	106	R		H	0.1305	0.00553	2448.8
1324	B				A2V	98	R			0.4692	0.03117	4978.2
1330	PB	138–152			A7V	79	R			0.3023	0.02542	1872.0
1341	PB	35–44			A0pSi	97	R			0.1606	0.02224	1288.9
1342	S	130–145			A3V	95	R			0.02325	0.00856	322.7
1368	SB				A3m	46	R	P		0.02448	0.0	32.6
1376	SB				A1m	47	R			0.02222	0.00919	38.6
1380	SB				A7V	45	R			0.03143	0.00932	101.1
1389	B		1.3/63	3.3/4.5	A2IV	45	R		H	0.01973	0.00188	51.7
1412	SB				A7III	46		P		0.02410	0.0	361.1
1438	B		30	3	A2V	123	R			0.05492	0.02248	532.2
1458	SB				A5m	46	R		H	0.05959	0.00385	632.5
1466	B		0.3/0.8	0.8/1.6	A8V	85	R		H	0.01630	0.00179	524.6
1473	SB				A6V	46	R			0.02527	0.01011	46.0
1490	B		43	5	A2V	103	R			0.09877	0.01624	975.0
1501	PB	73–85			A8V	72	R			0.02963	0.00966	144.8
1511	B		<1	4	A3m	50	R			0.02433	0.00904	40.6
1522	PB	120–132			A2V	85		P		0.00677	0.0	35.1
1530	PB				A8/A9III/IV	68		P		0.0	0.0	[1]
1568	SB		<1	3.4	A1V	115	R			0.1428	0.02016	2088.7
1592	B		4.5	3	A1V+G0-2V	49	R		H	0.1872	0.01070	1656.2
1639	B		0.3	2.9	A5V+G2-5V	82	R			0.02810	0.00931	170.2
1664	B		0.7	0.8	Am+A5-F0V	59	R			0.03835	0.01250	73.5
1666	B	177–200			A3III	27	R			0.1763	0.02362	—
1670	B	30–87	11.8	2.7	A5m+M2V	55	R			0.03316	0.00977	109.8
1734	B	111–124	4.1	6	A7V+K5-M0V	72	R	P		0.02300	0.00181	109.8
1857	B		1.5	3.5	A0V+G0V	114	R			0.04920	0.01299	667.1
1872	PB	140–154			A2V	106	R			0.03153	0.00994	364.1
1971	PB	21–29			A2VpCr	148		P		0.0	0.0	[2]
2015	S	172–225			A7V	44		P	H	0.00609	0.00139	3.6
2020	S	104–130			A5V	19			H	0.00131	0.00031	1.4
2088	B	32–41	12.6	12.2	A2IV	25			H	0.01018	0.00186	18.5
2095	B		2.2/	4.5/	A0pSi+F2-5V	53	R			0.1186	0.01951	94.9
2124	SB				A2V	47	R	P	H	0.1245	0.00359	180.3
2181	B	248	0.1	0.1	A0V+A	80	R			0.02450	0.00744	184.3
2238	PB	35–47			A2Vs	46	R			0.01886	0.00877	35.1
2253	B		2.3/25.4	5.3/7	A3V+G2-5V	195	R			0.02084	0.00915	1292.0
2280	B		0.4	0.5	A4.5V	102	R			0.03662	0.01048	411.2
2298	SB		14/93.6	2.3/8.3	A5IV	39	R		H	0.01297	0.00426	85.7
2320	PB				Am	50	R			0.01822	0.00451	42.9
2328	B	220–238	21.1	2.4	A0Vn	125	R			0.1372	0.01845	2640.5
2421	SB				A0IV	32	R		H	0.06328	0.00555	220.5
2424	B		1.5/21.5	0.8/5.5	A0V+A0V	178	R		H	0.02561	0.00201	2209.4
2466	PB	90–102	0.0055	2.4	A2V	43	R			0.09255	0.01812	125.0
2482	B		8	1.5	A3V	91	R			0.04727	0.01076	259.1
2491	SB				A1V	3	R		H	2.584	0.02469	66.7
2550	PB	206			A7IV	30	R	P		0.08366	0.00296	65.2
2626	SB				A0V	130	R			0.01559	0.00698	191.3
2890	SB				A2Vm	16	R		H	0.3086	0.00202	830.4
2891	SB				A1V	16	R		H	0.3086	0.00202	226.8
2950	B		0.9		A0III	—		P		0.00514	0.00164	—
3173	B		45.6/7.3	8/0.5	A2V+M0V	67	R			0.02640	0.01003	104.6
3221	B		2.8/48.6/+	3.2/...	A7Vm	153	R			0.01983	0.00991	340.9

[1] Simon et al. (1995) calculate an L_x of 33×10^{27} erg/s from PSPC pointing observations. The Second ROSAT Source Catalog of Pointed Observation (2001) lists false detections in the field and therefor no count rate for the source.

[2] In The Second ROSAT Source Catalog of Pointed Observation (2001) this source is flagged as suspect in lightcurve, variability and spectrum. No count rate for the source is listed.

Table 3. continued.

HR	Binary	$v \sin(i)$	Sep.	δ mag	Components	Distance	Catalog			CR	±CR	L_{x27}
3260	B		3.6	2.6	A2V+F2V	74	R			0.09536	0.01760	535.5
3314	S	115–161			A0V	38			H	0.00639	0.00157	27
3337	SB		0.17		A5m	85	R		H	0.03410	0.00463	1172.2
3352	SB		1.8	3.3	A2m	84	R			0.05309	0.01266	328.3
3410	SB				A1Vnn	55	R			0.1015	0.02102	218.9
3455	B		3.8	2	A3V	70	R			0.5313	0.05003	2994.4
3460	B		21.4	9.8	A0V	73	R			0.03332	0.01167	214.3
3485	B		0.6/2.6	/3	A1V	24	R		H	0.1047	0.00888	134.0
3524	B				A8V+A8V	98	R		H	0.01935	0.00161	2985.0
3569	SB		10.7		A7IV	15	R		H	0.04752	0.00520	28.2
3586	B	170–186	0.53	3.2	A9Vn	66		P		0.01903	0.0	587.4
3655	B				A3III+A0V	83	R			0.03523	0.01223	271.2
3685	S	145–167			A2IV	34			H	0.00781	0.00090	26.1
3690	SB				A3V	37	R			0.2099	0.02384	206.2
3699	PB	10			A8Ib	212	R			0.05838	0.01893	464.6
3756	B		0.1	0.1	A5III/IV	115	R			0.06428	0.01169	930.5
4065	B	183	2	0.1	A1V	89	R			0.06759	0.01836	574.6
4096	B		1.7	4	A2V	66	R			0.03358	0.01125	131.3
4203	PB		200		A1Vn	116	R			0.02432	0.01012	278.2
4228	S				A0Ia	—		P		0.03660	0.00399	—
4229	B		1.9	0.6	A2IV	96	R			0.03664	0.01580	300.4
4237	B		27.3	5.8	A3m	112			H	0.00438	0.00072	158.8
4296	B		10.6	7.3	A3III-IV	60		P		0.01840	0.0	46.3
4309	B		8.2	5.6	A3III-IV	81			H	0.00536	0.00059	100
4343	B	40–49			A1V+WD	82	R			0.4689	0.04332	2262.8
4350	S				A3IV-V	50	R			0.07834	0.02435	204.1
4380	SB				A2V+A1V	56	R			0.05317	0.01638	122.8
4385	B		<1	3.4	A8IIIm	65	R			0.02670	0.00774	78.5
4405	B		5.2	3.8	A9V	26	R	P		0.02455	0.0	13.1
4422	SB		5.5		A2V	64	R			0.05441	0.01684	195.6
4454	B		<1	2.8	A2m+F8-G0	114	R			0.05492	0.01434	565.5
4528	B		0.3		A1	59	R			0.01922	0.00858	84.9
4535	SB				A3m	63	R			0.02716	0.01110	119.9
4574	B		7.4	6.1	A9V	47			H	0.00499	0.00234	32.2
4599	SB		4.5	9.5	Am	70	R			0.02888	0.01095	81.4
4646	SB				A5m	34	R			0.2709	0.05984	274.2
4703	B		32	5.7	A5V+G8-K0V	103		P		0.01230	0.00384	93.7
4717	PB				A3V	87		P		0.00576	0.00088	31.7
4791	SB		20.3	1.5	A3III-IV	806			H	0.00078	0.00047	—
4796	B		6.9	7.5	A0V	67	R	P	H	0.1107	0.00457	428.4
4855	S		139	3.2	A3V	75	R	P		0.1126	0.0	281.5
4892	SB		22		A0V+A2V+HR4893	68	R			0.01271	0.00541	42.3
4915	SB		20		A0pSiEuHg	34	R			0.07636	0.01479	62.6
4921	B		0.1/20.9	/4.3	A3V	91		P		0.02245	0.0	133.4
5037	PB	205–222			A2V	65	R	P		0.2937	0.00919	1149.8
5054	SB				A2V	24	R	P		0.02818	0.00269	8.6
5055	SB				A1m	—	R	P		0.02172	0.00259	—
5144	B		4.8	3	A1V	93	R		H	0.03321	0.00324	869.5
5234	B		1.5/27.9	0.8/6.4	A1V	143		P		0.04743	0.00848	1127.4
5269	S				ApSi	169			H	0.00088	0.00045	72
5291	SB				A0III	95	R			0.04237	0.00972	274.4
5350	SB				A9V	30	R			0.05820	0.01190	36.0
5360	S				A2IV	102			H	0.00797	0.00254	236.3
5386	B		6.1/	1.7/0.3	A0V+F0V+F2V	66	R			0.08158	0.01807	273.5
5401	B		26.9	5.7	Am	58	R			0.02251	0.01012	48.8
5413	SB		22	5.5	A1V	68	R		H	0.01965	0.00095	690.3
5433	B		2	9.8	A7Vn	71	R			0.04928	0.01152	245.3
5663	B		13.3	4.4	A3m	52	R			0.01862	0.00857	30.9
5697	B		5.7	2.2	A0pSi+F5-8V	123	R		H	0.03590	0.00405	2409.4
5719	B		1.4	5.5	A0pSi	118	R	P		0.05763	0.0	1601.4
5756	SB		11	2.7	A2V	73	R			0.02947	0.01199	112.7
5765	B		9.2/?	1.2/1.4	A4V	102	R			0.07019	0.01404	1160.5
5793	B				A0V+G5V	23	R	P	H	0.1324	0.00681	51.5
5818	B		?	?	A2V	76	R	P		0.06149	0.00519	443.6
5846	B		3.7	1.8	A0V+B	141	R			0.1035	0.01961	2006.2
5887	SB		1.3	3	A3m	80	R			0.01645	0.00533	78.3
5895	B	185–229	0.1		A3Vn	49	R	P		0.04194	0.0	50.9
5961	B		0.2/10	0.5/2.4	A7IV	43	R		H	0.4617	0.01690	3566.3
5983	SB				A2III+G8	212	R			0.03313	0.01155	1066.8
5999 [3]	SB				A7IVe	208	R	P	H	0.2870	0.01450	20422.5
6000	B		1.3	4.6	A1III	241	R	P	H	0.1892	0.00595	3902.4
6097	B		6.2	0.4	A0V+A0V	117	R			0.07391	0.01681	1009.1
6111	SB				A1III+M	105	R			0.02651	0.01026	473.1
6123	B		0.2		A5V	79	R			0.01403	0.00557	123.1
6129	SB		0.8	3.2	A3m	37	R			0.2882	0.02920	372.0
6162	B		16.3	3.3	A4Vn	69	R			0.04089	0.00916	155.2
6186	B		3.7	1	A1Vnn	122	R			0.07209	0.01542	418.2
6216	B		1.9/24	3.5/7.4	A2V	92	R			0.03966	0.01394	208.8
6218	B		5.4	7.6	A3IV	231	R			0.01908	0.00957	1438.3
6240	SB				A7+F6	74	R	P	H	0.4669	0.00742	1344.3
6254	B		1.8/	5.5/	A2VpSrCrEu	54	R		H	0.01402	0.00263	90.7
6317	SB		0.1		A7V	73	R			0.01663	0.00700	144.2
6377	B		0.08/19.5	0/6	A5m	54	R			0.02051	0.00739	42.9

[3] See Zinnecker & Preibisch (1994) and Hamaguchi et al. (2005).

Table 3. continued.

HR	Binary	$v \sin(i)$	Sep.	δ mag	Components	Distance	Catalog			CR	±CR	L_{x27}
6435	B	210–228	1.6/11.5	1/4.9	A0V(nn)	114	R		H	0.04231	0.00238	1390.6
6436	SB		0.9		A2V	55	R	P		0.03320	0.0	92.5
6554	SB		60		A6V	30	R			0.01433	0.00427	9.7
6555	SB				A4m	31	R			0.01433	0.00427	9.9
6556	PB				A5III	14	R			0.1241	0.01652	18.3
6618	PB	130–170			A2V	127	R			0.00979	0.00324	207.7
6641	SB		0.1		A2Vs	132	R			0.08195	0.00874	1661.5
6656	B				A2V	67	R			0.00915	0.00344	65.6
6730	B		6.1	0.2	A5IIIn	144	R			0.1143	0.01617	1680.3
6771	SB		25.3/51.7	10.3/7.3	A4IVs	25	R			0.02134	0.00982	8.6
6781	B		0.1/14.2		A3V	70	R		H	0.09434	0.00861	2239.4
6825	PB	25–33			ApSi	1205	R			0.05331	0.01705	–
6843	B		0.7	3.5	A8V	132	R			0.1390	0.02396	3939.3
6876	SB				A5m	58	R			0.04933	0.01029	145.0
6923	SB				A1V	58	R	P	H	0.06139	0.00518	373.0
6956	B		<0.1		A4-5IV/V	74	R			0.04510	0.01560	248.8
7001	B		43/46	9.5/11	A0Va	8			H	0.1125	0.00514	19.4
7051	B		3.4	0.9	A4V	50	R	P	H	0.07280	0.00424	189.1
7056	SB				A4m	47	R			0.2511	0.02232	571.6
7077	B		0.2		A1m	128	R			0.02421	0.01161	649.4
7124	SB				A1Vn	93	R			0.02501	0.00495	203.5
7160	S				A8V	88	R	P	H	0.04693	0.00536	243.4
7214	PB				A4V	55	R			0.07833	0.01560	255.2
7215	B		41.9	5.6	A7V	39	R			0.07750	0.01322	105.3
7235	SB				A0Vn	26	R		H	0.05526	0.00451	84.9
7313	PB	195–212			A1Vn	84	R			0.04254	0.01231	255.3
7392	SB				Am	57	R			0.03887	0.01431	122.3
7431	SB				A1mA2-F0	89	R		H	0.01046	0.00326	134.9
7557	S				A7V	5	R	P		0.1785	0.00357	6.4
7562	B		0.4	3.3	A1m	117	R	P		0.0264	0.0	370.2
7571	B		0.15		A1V+F8IV	117	R			0.3836	0.04335	6865.9
7610	SB				A1IV	63	R	P		0.03413	0.0	122.1
7695	B		4.9/150	3–4/5	A2II-III+	78	R			0.02284	0.00550	101
7755	B		0.2		A2Vn	109	R			0.00606	0.00297	52.6
7775	SB				B9.5III/IV	96	R			0.02685	0.01216	177.6
7781	SB		3		A2Vs	89	R			0.03763	0.00656	291.8
7917	SB		1.2	3	A2V	82	R			0.01681	0.00727	128.0
8021	SB				A7III+G2III	45	R			1.024	0.07911	1802
8028	B		0.2		A1Vne	109	R			0.04808	0.01015	788.3
8060	B		0.3	1.3	A5V	48	R			0.04937	0.01884	188.4
8101	B		17.9	1	A1V	621	R			0.06809	0.01332	—
8140	B		3	2.5	A5V+G0V	30	R		H	0.1034	0.00936	341.3
8151	B		0.15	2.5	A2pCrEuSr+	57	R			0.1062	0.01907	411.2
8162	B		209.2	8	A7IV	15	R	P		0.02026	0.00278	7.1
8210	SB				A8Vm+WD	46	R			1.052	0.06780	3631.1
8263	B		31.3	3.3	A2V	122	R			0.02600	0.01072	322.3
8266	PB	185–201			A5V	63	R			0.01405	0.00626	36.6
8307	B		1.4/	5.4/	A0V	84		P		0.05806	0.00468	4326.6
8322	B				Am	12	R			1.655	0.12550	187.5
8396	SB				A2V+K0III	145	R		H	0.03348	0.00316	505.2
8417	SB				A3m	31	R		H	0.05639	0.00470	169.7
8431	PB				A2V	40	R			0.03442	0.01345	89.6
8518	SB				A0V	48	R			0.05508	0.01707	92.9
8533	B		0.5/	0.2/	A0V	130	R	P		0.01041	0.0	448.2
8576	B		30.3	2	A0V	45	R			0.06447	0.01814	88.5
8598	B		9.5/	3/	A0V	123	R			0.01753	0.00758	104.9
8600	PB				A3Vn	69	R			0.03796	0.01648	169.9
8662	SB				A9IIIm	74	R		H	0.00376	0.00108	14.8
8724	B		3.9	2.9	A3Vs	82	R			0.04692	0.01266	337.9
8738	S				A1V	96		P		0.01433	0.00	90.2
8799	S				A5V	40	R			0.02123	0.00783	14.7
8865	B		1.2	4	A0V	76	R		H	0.07713	0.00658	834.0
8884	B		13.2	3.5	A5Vn	80	R			0.01986	0.00827	121.2
8963	B		27.7	6.2	A1Vn	73			H	0.00203	0.00086	31.3
9016	B		3.3/	7/	A0V	44	R	P	H	0.1724	0.00813	379.4
9039	PB	156–180			A4Vn	58	R			0.03021	0.01058	99.6